BJR

https://doi.org/10.1259/bjr.20170580

Received: 10 August 2017 | Revised: 14 December 2017 | Accepted: 14 December 2017

Cite this article as:
Kong L-Y, Zhang W, Zhou Y, Xu H, Shi H-B, Feng Q, et al. Histogram analysis of apparent diffusion coefficient maps for assessing thymic epithelial tumours: correlation with world health organization classification and clinical staging. *Br J Radiol* 2018; **91**: 20170580.

FULL PAPER

Histogram analysis of apparent diffusion coefficient maps for assessing thymic epithelial tumours: correlation with world health organization classification and clinical staging

[1]LING-YAN KONG, MS, [1]WEI ZHANG, PhD, [2]YUE ZHOU, [1]HAI XU, PhD, [1]HAI-BIN SHI, MD,PhD, [3]QING FENG, MD,PhD, [1]XIAO-QUAN XU, PhD and [1]TONG-FU YU, MD, PhD

[1]Department of Radiology, The First Affiliated Hospital of Nanjing Medical University, Nanjing, China
[2]Department of Thoracic Surgery, The First Affiliated Hospital of Nanjing Medical University, Nanjing, China
[3]Department of Nutrition and Food Hygiene, School of Public Health, Nanjing Medical University, Nanjing, China

Address correspondence to:
Prof Tong-fu Yu
E-mail: *njmu_yutongfu@163.com*
Prof Xiao-Quan Xu
E-mail: *xiaoquanxu_1987@163.com*

The authors Ling-Yan Kong, Wei Zhang, Yue Zhou and Hai Xu contributed equally to the work

Objective: To investigate the value of apparent diffusion coefficients (ADCs) histogram analysis for assessing World Health Organization (WHO) pathological classification and Masaoka clinical stages of thymic epithelial tumours.

Methods: 37 patients with histologically confirmed thymic epithelial tumours were enrolled. ADC measurements were performed using hot-spot ROI (ADC_{HS-ROI}) and histogram-based approach. ADC histogram parameters included mean ADC (ADC_{mean}), median ADC (ADC_{median}), 10 and 90 percentile of ADC (ADC_{10} and ADC_{90}), kurtosis and skewness. One-way ANOVA, independent-sample *t*-test, and receiver operating characteristic were used for statistical analyses.

Results: There were significant differences in ADC_{mean}, ADC_{median}, ADC_{10}, ADC_{90} and ADC_{HS-ROI} among low-risk thymoma (type A, AB, B1; n = 14), high-risk thymoma (type B2, B3; n = 9) and thymic carcinoma (type C, n = 14) groups (all p-values <0.05), while no significant difference in skewness (p = 0.181) and kurtosis (p = 0.088). ADC_{10} showed best differentiating ability (cut-off value, ≤0.689 × 10^{-3} mm^2 s^{-1}; AUC, 0.957; sensitivity, 95.65%; specificity, 92.86%) for discriminating low-risk thymoma from high-risk thymoma and thymic carcinoma. Advanced Masaoka stages (Stage III and IV; n = 24) tumours showed significant lower ADC parameters and higher kurtosis than early Masaoka stage (Stage I and II; n = 13) tumours (all p-values <0.05), while no significant difference on skewness (p = 0.063). ADC_{10} showed best differentiating ability (cut-off value, ≤0.689 × 10^{-3} mm^2 s^{-1}; AUC, 0.913; sensitivity, 91.30%; specificity, 85.71%) for discriminating advanced and early Masaoka stage epithelial tumours.

Conclusion: ADC histogram analysis may assist in assessing the WHO pathological classification and Masaoka clinical stages of thymic epithelial tumours.

Advances in knowledge: 1. ADC histogram analysis could help to assess WHO pathological classification of thymic epithelial tumours. 2. ADC histogram analysis could help to evaluate Masaoka clinical stages of thymic epithelial tumours. 3. ADC_{10} might be a promising imaging biomarker for assessing and characterizing thymic epithelial tumours.

INTRODUCTION

Thymic epithelial tumours are the most common primary neoplasms in the anterior mediastinum.[1] World Health Organization (WHO) divides thymic epithelial tumours into low-risk thymoma (types A, AB, B1), high-risk thymoma (type B2, 3) and thymic carcinoma (type C), based on morphology of epithelial cells and ratios of lymphocytes to epithelial cells.[2] Clinical stages of thymic epithelial tumours are usually analysed based on the Masaoka-Koga staging system according to surgical findings.[3] Accurate pre-treatment assessment of WHO classification and clinical staging are crucial because this

information influences the surgical planning.[4] Therefore, an effective and objective approach to assess the WHO classification and clinical staging of thymic epithelial tumours prior to treatment is urgently needed.

CT and MR imaging are commonly used for delineating anterior mediastinal masses.[1,3] Despite their irregular contour, necrotic or cystic components, heterogeneous enhancement, lymphadenopathy and great vessel invasion on conventional CT or MR images strongly suggest thymic carcinoma, the value of qualitative image features for differentiating different subtypes of WHO classification is still controversial.[1,4] Also, qualitative assessment of imaging features is subjective, and suffers from inter-reader variability.

Recently, several quantitative MR imaging techniques have been used for assessing thymic tumours, including diffusion-weighted imaging (DWI),[5] intravoxel incoherent motion DWI,[6] dynamic contrast-enhanced MR imaging[7] and chemical-shift MR imaging.[8] Among these techniques, DWI was most commonly used due to its simplicity, and lack of need for contrast media. Its derived apparent diffusion coefficient (ADC) has been proven to be useful for differentiating malignant from benign masses in paediatric and adult patients, and in assessing the WHO classification and clinical staging of thymic epithelial tumours.[4,5,9–11] However, they placed regions of interest on three selected slices of the tumours and only mean ADC value was derived, which could not totally reflect tumour heterogeneity. By contrast, processing DWI data using a histogram approach may be useful for providing quantitative information about tumour heterogeneity.[12] It has showed superiority to previous selected ROIs approach in differentiating and grading tumours in various organs.[13,14] However, the study that applies histogram analysis of ADC maps in assessing and characterizing thymic epithelial tumours is still limited.

Therefore, the purpose of this study is to evaluate the value of histogram analysis of ADC maps in assessing the WHO classification and Mosoaka clinical staging system of thymic epithelial tumours.

METHODS AND MATERIALS

Patients

This study was approved by the institutional review board of our hospital, and informed consent was waived due to retrospective nature of the study. From May 2015 to November 2016, 70 patients with histologically confirmed mediastinal tumours underwent MR imaging (including DWI) for pre-treatment evaluation. Among these 70 patients, 33 patients were excluded because of the following criterions: (1) previous biopsy before MRI scan (n = 5); (2) the image quality of DWI was not adequate for further analysis (n = 6) and (3) the diagnosis was not thymic epithelial tumours (n = 22). Finally, we enrolled 37 patients with thymic epithelial tumours (17 males and 20 females; mean age, 53 years; range, 30–76 years) into our study.

37 thymic epithelial tumours including 23 thymomas (including 2 type A, 9 type AB, 3 type B1, 6 type B2, 3 type B3) and 14 thymic carcinomas (type C) were stratified according to WHO classification into low-risk thymoma (n = 14), high-risk thymoma (n = 9) and thymic carcinoma (n = 14). The Masaoka clinical stages for 37 thymic epithelial tumours were Stage I (n = 4), Stage II (n = 10), Stage III (n = 10) and Stage IV (n = 13).

MR imaging scan

All MR imaging studies were performed with 3T MR system (Verio, Siemens, Erlangen, Germany). All patients underwent axial T_1 weighted imaging, coronal T_2 weighted imaging and single-shot spin echo-planar imaging-based DWI. Imaging variables were summarized in Table 1.

Image analysis

All DWI data were processed offline using in-house software (FireVoxel; CAI^{2}R, New York University, NY) using a mono-exponential model.[15,16] During ADC histogram analysis, ROIs were manually drawn on the image slices which encompassed as much tumour area. With reference to T_2 weighed image, large fatty, necrotic, cystic, and haemorrhagic areas were excluded. After ROIs were drawn, histogram analysis was performed. ADC histograms were plotted with diffusivity on the X-axis with a bin size of 1×10^{-3} mm^2 s^{-1}, and the Y-axis expressed the percentage of tumour volume by dividing the frequency in each bin by the total number of voxels analysed. We evaluated four representative parameters, including mean ADC (ADC_{mean}); median ADC value (ADC_{median}), skewness and kurtosis. Kurtosis, which is a measure of histogram peakedness: values are equal to 3 when the histogram is Gaussian, >3 with a sharper peak, and <3 with a flatter top. Skewness, which is a measure of the asymmetry of the histogram, is positive if the majority of the data is concentrated on the left of the histogram and negative if the majority of data is concentrated on the right.[17] We also measured two cumulative histogram variables including the 10 and 90 percentiles of ADC (ADC_{10} and ADC_{90}). The nth percentile was the point at which

Table 1. MR scan protocol and imaging variables

Variables	T_1 weighted imaging	T_2 weighted imaging	Diffusion-weighted imaging
Plane	Axial	Coronal	Axial
Repetition time (ms)	140	1200	6600
Echo time (ms)	2.5	93	76
Field of view (cm)	36	36	36
Slice thickness (mm)	5	5	4
Matrix	320 × 180	384 × 246	144 × 117

Figure 1. A representative case for introducing two different ROIs selection methods. (a) During hot-spot ROIs based ADC measurements, three circular ROIs (about 0.5 cm^2) were placed on the tumours area which showed increased signal intensity on DW image (b_{1000}). (b) During histogram-based ADC measurements, ROIs were manually drawn on all image slices encompassing as much as tumour area. The selection method in a typical slice is shown.

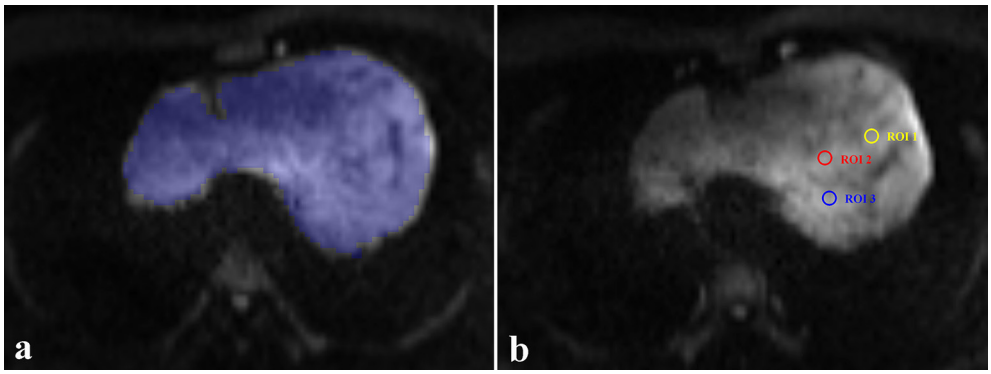

n% of the voxel values that form the histogram were found on the left.[18]

During ADC measurements based on hot-spot ROIs, the slice on which the tumour showed the biggest diameter was chosen. Three circular ROIs (about 0.5 cm^2) were placed on tumour area which demonstrate mostly increased signal intensity on DW image (b_{1000}). Large fatty, necrotic, cystic, and haemorrhagic areas were excluded. The measured ADCs from the three ROIs were averaged to a mean ADC ($ADC_{HS\text{-}ROI}$) for statistical analyses. The average time for ADC histogram analysis and ADC measurements based on hot-spot ROIs were 95.3 ± 28.5 and 30.6 ± 9.2 s. A representative case for introducing two ROIs selection methods during hot-spot ROIs based and histogram-based ADC measurements is showed in Figure 1.

Both histogram-based and hot-spot ROI-based ADCs measurements were determined by two dedicated radiologists (reader 1: with 5 years of clinical experience; reader 2: with 2 years of clinical experience), blinded to the study design. The measurements of two radiologists were used to evaluate inter-reader reproducibility. To evaluate intrareader reproducibility, reader 1 performed all the measurements again after at least 1e month after the first measurement. The average of the two measurements from reader 1 was used for statistical analyses.

Statistical analysis

Continuous variables were reported as mean ± standard deviation, and tested for normality using Kolmogorov–Smirnov test. One-way ANOVA was used to compare the differences in patient age and ADC variables among low-risk thymoma, high-risk thymoma and thymic carcinoma groups. χ^2 test was used to compare the difference of gender. Independent-sample *t*-test was used to compare ADC variables between early stage (Masoaka-Koga Stage I and II) and advanced stage (Masoaka-Kog Stage III and IV) thymic epithelial tumours. Receiver operating characteristic (ROC) curves analyses were used to assess the diagnostic performance of significant variables for differentiating low-risk thymoma from high-risk thymoma and thymic carcinoma, and in differentiating early from advanced stage thymic epithelial tumours. The area under the ROC curves (AUCs) were compared using the method of Delong et al.[19]

Intraclass correlation coefficients (ICCs) were used to explore the inter- and intrareader reproducibility of ADC

Table 2. Histogram variables among low-risk thymoma, high-risk thymoma and thymic carcinoma

Variables	Low-risk thymoma (*n* = 14)	High-risk thymoma (*n* = 9)	Thymic carcinomas (*n* = 14)	*p*-value
ADC histogram				
ADC_{mean}	1.301 ± 0.056	1.195 ± 0.049	1.169 ± 0.181	0.016
ADC_{median}	1.256 ± 0.052	1.166 ± 0.043	1.142 ± 0.179	0.039
ADC_{10}	0.837 ± 0.115	0.631 ± 0.087	0.579 ± 0.099	<0.001
ADC_{90}	1.874 ± 0.203	1.667 ± 0.168	1.574 ± 0.213	0.001
Skewness	0.741 ± 0.373	0.705 ± 0.274	0.929 ± 0.213	0.181
Kurtosis	4.108 ± 1.072	4.706 ± 1.027	5.019 ± 1.087	0.088
$ADC_{HS\text{-}ROI}$	1.123 ± 0.091	1.127 ± 0.047	1.097 ± 0.221	0.045

Except *p* value, data are reported as mean ±standard deviation. ADC indicates apparent diffusion coefficient.
ADC*n*, *n*th percentile value of cumulative ADC histogram. The unit of ADC value is $\times 10^{-3}$ mm^2 s^{-1}.

Figure 2. Representative images of patients with low-risk thymoma (a–e), high-risk thymoma (f–j) and thymic carcinoma (k–o). First column were axial T_1 weighted image of a 46-year-old female patient with type AB thymoma (a), that of a 48-year-old female patient with type B2 thymoma (f), and that of a 42-year-old male patient with thymic carcinoma (k). After ROIs were placed (b, g and l), coloured ADC maps were conducted and embedded into diffusion images (b_{1000} map) (c, h and m). Corresponding histogram maps showed lower ADC value for thymic carcinoma (n), followed by high-risk thymoma (i) and low-risk thymoma (d). All diagnoses were confirmed by histological examination (e, j and o).

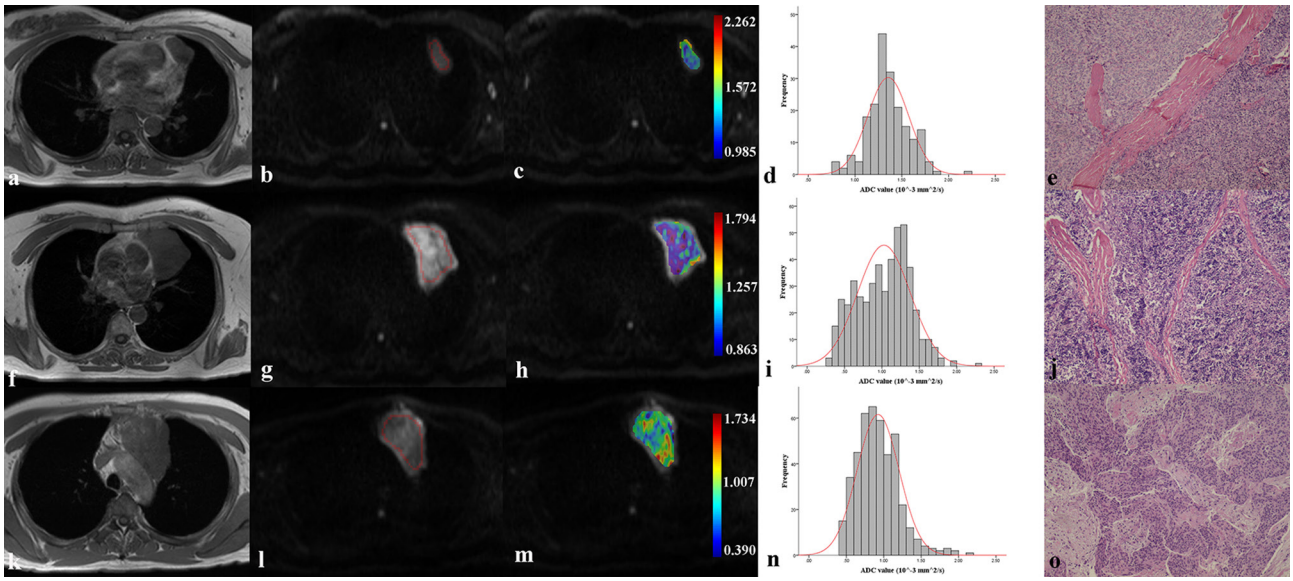

measurements. ICC ranged between 0 and 1.00, and values closer to 1.00 represented better reproducibility. Values of 0.20 or less indicated poor reproducibility, 0.21–0.40 indicated fair reproducibility, 0.41–0.60 indicated moderate reproducibility, 0.61–0.80 indicated good reproducibility and 0.81 or higher indicated excellent reproducibility.[17] Statistical analyses were performed with SPSS v. 17.0 (SPSS software, Chicago, IL) or MedCalc v. 11.5 (MedCalc Software, Mariakerke, Belgium). Significant threshold for difference was set at a two-sided p-value of less than 0.05.

RESULTS

There were no significant differences in age ($p = 0.112$) and sex ($p = 0.333$) among low-risk thymoma, high-risk thymoma and thymic carcinoma groups. There were significant differences on the ADC_{mean}, ADC_{median}, ADC_{10}, ADC_{90}, and $ADC_{HS\text{-}ROI}$ among three groups (all p-values <0.05), while no significant differences on skewness ($p = 0.181$) and kurtosis ($p = 0.088$) (Table 2). Representative images of patients with low-risk thymoma, high-risk thymoma and thymic carcinoma were showed in Figure 2.

ADC_{10} showed best differentiating ability for differentiating low-risk thymoma from high-risk thymoma and thymic carcinoma [cut-off value, $\leq 0.689 \times 10^{-3}$ mm^2 s^{-1}; AUC, 0.957; sensitivity, 95.65%; specificity, 92.86%] (Table 3), followed by ADC_{median}, ADC_{mean}, ADC_{90} and $ADC_{HS\text{-}ROI}$(Figure 3). For multiple comparisons of ROC curves, ADC_{10} showed significant higher AUC than $ADC_{HS\text{-}ROI}$ ($p = 0.029$), while no significant differences were found for any other comparisons (all p-values >0.05).

Advanced stage tumours showed significant lower ADC variables and higher kurtosis than early stage tumours (all p-values

Table 3. Diagnostic performance of histogram variables for differentiating low-risk thymoma from high-risk thymoma and thymic carcinoma

Variables	Cut-off value	AUC	Sensitivity (100%)	Specificity (100%)
ADC histogram				
ADC_{mean}	1.268	0.857 (0.731–0.983)	91.30 (72.0–98.9)	71.43 (41.9–91.6)
ADC_{median}	1.221	0.870 (0.750–0.990)	86.96 (66.4–97.2)	78.57 (49.2–95.3)
ADC_{10}	0.689	0.957 (0.881–1.000)	95.65 (78.1–99.9)	92.86 (66.1–99.8)
ADC_{90}	1.608	0.823 (0.691–0.955)	60.87 (38.5–80.3)	92.86 (66.1–99.8)
$ADC_{HS\text{-}ROI}$	1.183	0.832 (0.690–0.974)	86.96 (66.4–97.2)	78.57 (49.2–95.3)

Data in parentheses indicate 95% confidence intervals. AUC indicates largest area under the ROC curve.
ADC, apparent diffusion coefficient; ADCn, nth percentile value of cumulative ADC histogram.

Figure 3. Receiver operating characteristic curves of using ADC_{HS-ROI}, ADC_{mean}, ADC_{median}, ADC_{10} and ADC_{90} for differentiating low-risk thymoma from high-risk thymoma and thymic carcinoma.

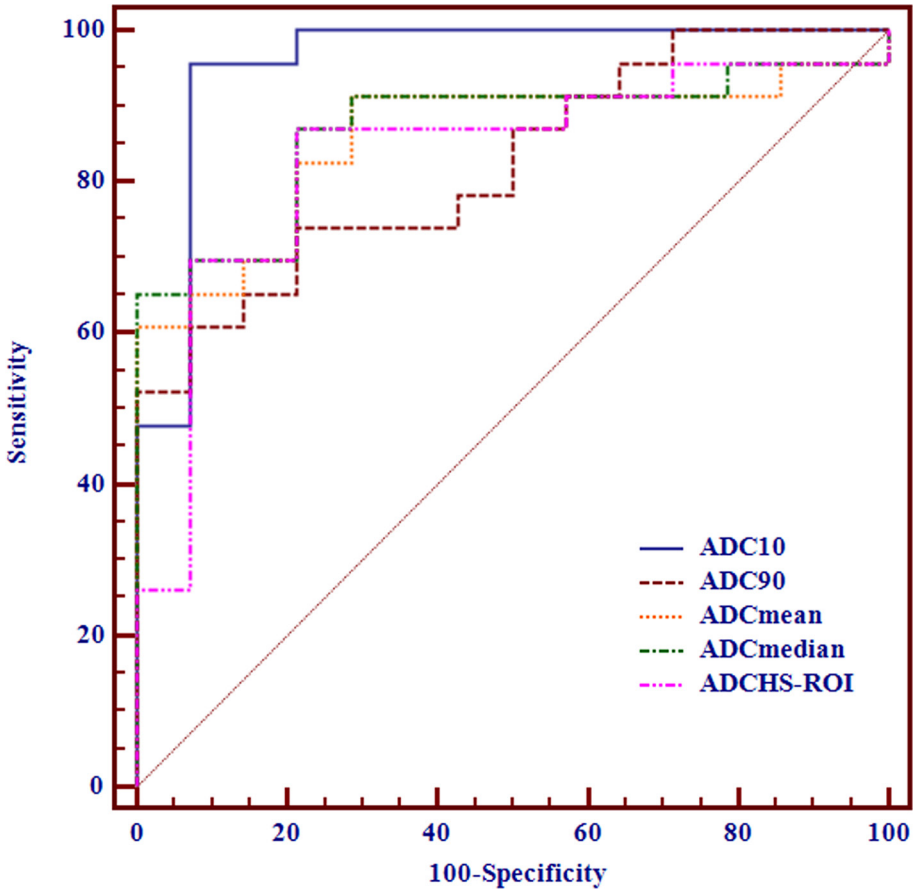

<0.05), while no significant difference was found on skewness (p = 0.063) (Table 4). ADC_{10} again showed best differentiating ability for differentiating early from advanced stage epithelial tumours (cut-off value, ≤0.689 × 10^{-3} mm^2 s^{-1}; AUC, 0.913; sensitivity, 91.30%; specificity, 85.71%) (Table 5), followed by ADC_{mean}, ADC_{median}, ADC_{90} and ADC_{HS-ROI} (Figure 4). For multiple comparisons of ROC curves, ADC_{10} showed significant higher AUC than ADC_{HS-ROI} (p = 0.034), while no significant differences were found on any other comparisons (all p-values >0.05).

Good to excellent inter- and intrareader agreements were obtained during ADC measurements. Inter and intrareader ICCs were 0.779 and 0.802 for ADC_{mean}, 0.772 and 0.803 for ADC_{median}, 0.780 and 0.794 for ADC_{10}, 0.769 and 0.782 for ADC_{90}, 0.772 and 0.788 for kurtosis, 0.767 and

Table 4. Histogram variables between early and advanced stage thymic epithelial tumours

Variables	Early stage (n = 13)	Advanced stage (n = 24)	p-value
ADC histogram			
ADC_{mean}	1.304 ± 0.053	1.177 ± 0.142	0.003
ADC_{median}	1.256 ± 0.052	1.152 ± 0.140	0.012
ADC_{10}	0.825 ± 0.124	0.607 ± 0.107	<0.001
ADC_{90}	1.889 ± 0.189	1.601 ± 0.193	<0.001
Skewness	0.676 ± 0.327	0.881 ± 0.305	0.063
Kurtosis	4.039 ± 0.996	4.939 ± 1.061	0.015
ADC_{HS-ROI}	1.229 ± 0.094	1.112 ± 0.175	0.028

Except p value, data are reported as mean ±standard deviation. ADC indicates apparent diffusion coefficient. ADCn, nth percentile value of cumulative ADC histogram. The unit of ADC value is ×10^{-3} mm^2 s^{-1}.

Table 5. Diagnostic performance of histogram parameters for differentiating early from advanced stage thymic epithelial tumours

Parameters	Cut-off value	AUC	Sensitivity (100%)	Specificity (100%)
ADC histogram				
ADC_{mean}	1.245	0.876 (0.754–0.997)	86.96 (66.4–97.2)	85.71 (57.2–98.2)
ADC_{median}	1.168	0.863 (0.742–0.985)	65.22 (42.7–83.6)	100.00 (76.8–100.0)
ADC_{10}	0.689	0.913 (0.816–1.000)	91.30 (72.0–98.9)	85.71 (57.2–98.2)
ADC_{90}	1.608	0.857 (0.738–0.976)	65.22 (42.7–83.6)	100.00 (76.8–100.0)
ADC_{HS-ROI}	1.183	0.792 (0.641–0.943)	82.61 (61.2–95.0)	71.43 (41.9–91.6)

Data in parentheses indicates 95% confidence intervals. AUC indicates largest area under the ROC curve.
ADC*n*, *n*th percentile value of cumulative ADC histogram.

0.793 for skewness, and 0.726 and 0.749 for ADC_{HS-ROI}, respectively.

DISCUSSION

Our study demonstrated that ADC histogram analysis could help to differentiate low-risk thymoma, high-risk thymoma and thymic carcinoma, as well as discriminate advanced from early Masaoka stages of thymic epithelial tumours. ADC_{10} might be a promising imaging biomarker for assessing WHO pathological classification and Masaoka clinical stages of thymic epithelial tumours.

Razek et al reported significant differences on mean ADC values among low-risk thymoma, high-risk thymoma and thymic carcinoma, or between early and advanced stage of tumours.[4] The cut-off mean ADC values for both readers used to differentiate low-risk thymoma from high-risk thymoma and thymic carcinoma were 1.25×10^{-3} mm^2 s^{-1} and 1.22×10^{-3} mm^2 s^{-1},

Figure 4. Receiver operating characteristic curves of using ADC_{HS-ROI}, ADC_{mean}, ADC_{median}, ADC_{10} and ADC_{90} for differentiating advanced from early stage thymic epithelial tumour.

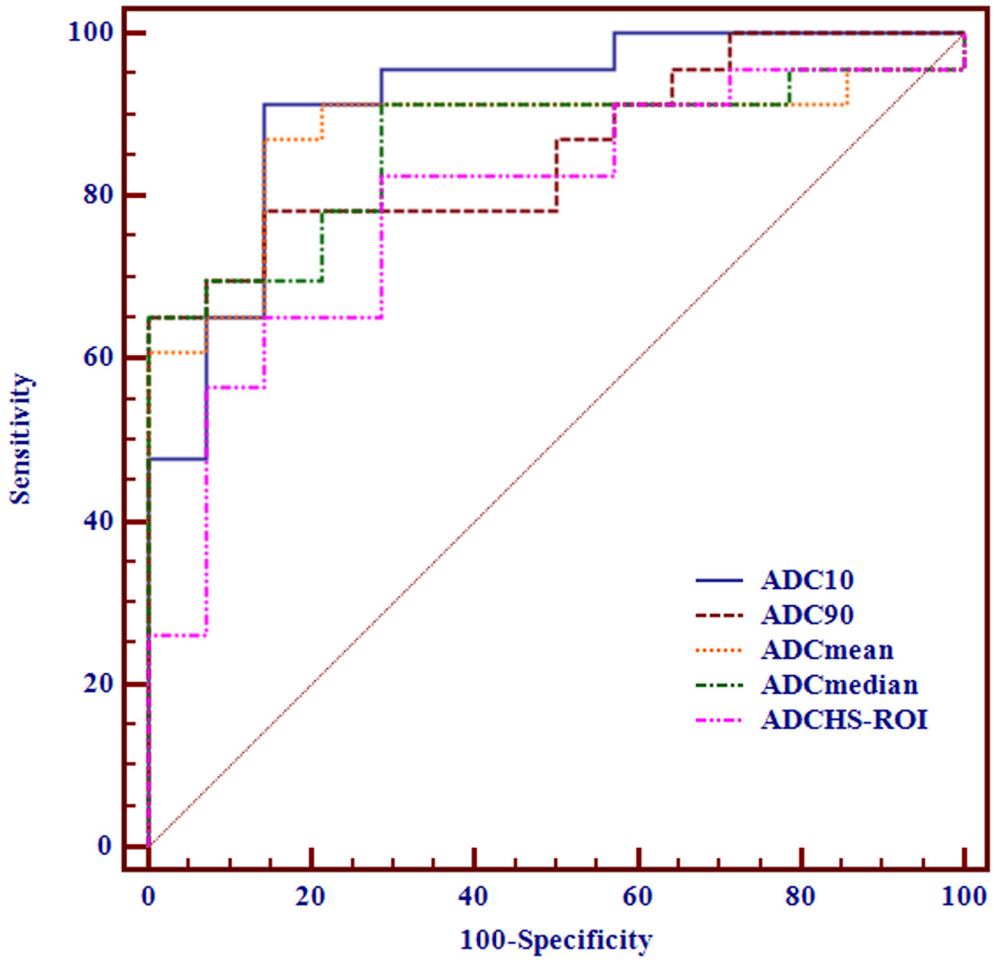

respectively. Similar change trend was also observed for ADC_{mean} in our study, suggesting that ADC value might be a potential imaging biomarker for differentiating different subtypes of thymic epithelial tumours. The cut-off value of ADC_{mean} was 1.268×10^{-3} mm^2 s^{-1}, which was slightly different from that of former study. This small difference might be associated with the difference in MR scanner (1.5 *vs* 3T) and MR acquisition variables (*b* value, 400/800 *vs* 1000 s mm^{-2}).

More important questions concerned by the clinicians is the discrimination of the clinical stage of thymic epithelial tumours, because of the impact association with the patient prognosis.[4] In our study, ADC_{10}, ADC_{90}, ADC_{mean} and ADC_{median} of advanced stage tumours were significantly lower than those of early stage tumours, and kurtosis of the former was higher than that of the latter one. This was because advanced Stage (III and IV) tumours were mostly high-risk thymoma and thymic carcinoma at histological examination, and subsequently demonstrated lower ADC and higher kurtosis than early stage tumours.

Due to its simplicity, hot-spot ROIs were commonly used for ADC measurements in clinical practice.[15] In our study, for differentiating different histological subtypes or clinical stages, ADC_{10} demonstrated better performance than $ADC_{HS\text{-}ROI}$. Similar findings about the superiority of low percentile of ADC value were also reported in previous studies.[16–18,20,21] Kang et al reported that the fifth percentile of ADC values obtained at a high *b* value DWI was the most promising parameter for differentiating high- from low-grade gliomas.[21] Compared with high percentile of ADC values that are more easily influenced by necrotic and cystic areas, low percentile of ADC values correlated well with areas of high cellularity. Therefore, low percentile of ADC value could reflect the difference of densely packed solid components within tumour tissue better than mean ADC value. Our study results indicated that ADC_{10} might be a promising imaging biomarker for differentiating pathological classifications and Masaoka clinical stages of thymic epithelial tumours in future applications.

Our study had several limitations. First, the study sample was limited. The limited sample size would increase the potential risk of statistical alpha and beta errors. Future studies with more patients are needed to confirm our results. Second, DWI image quality in about 8.6% (6/70) patients was inadequate for imaging analysis. Susceptibility artifacts associated with echo-planar imaging sequences were prominent for chest imaging. Third, compared with ADC_{10}, ADC_5 or minimum ADC value (ADC_{min}) might correlate better with solid tumour component. However, considering the greater noise-to-signal ratio of thoracic DWI, we did not choose ADC_5 or ADC_{min} as the imaging biomarker. Improvement of image quality will be the key to further studies. Fourth, our study data were derived from 3.0T field, and further work was required to validate our study results in other field strength. Finally, because of manual placement of ROIs, histogram analysis in our study was still a time-consuming process. Further optimization of the process of histogram analysis, and shorten of the processing time was needed.

In conclusion, our results suggested that ADC histogram analysis based on the entire tumour volume was a noninvasive, reliable and reproducible imaging method that may help to assess the WHO pathological classification and Masaoka clinical stage of thymic epithelial tumours. ADC_{10} may be a promising imaging biomarker for assessing and characterizing thymic epithelial tumours.

REFERENCES

1. Sadohara J, Fujimoto K, Müller NL, Kato S, Takamori S, Ohkuma K, et al. Thymic epithelial tumors: comparison of CT and MR imaging findings of low-risk thymomas, high-risk thymomas, and thymic carcinomas. *Eur J Radiol* 2006; **60**: 70–9. doi: https://doi.org/10.1016/j.ejrad.2006.05.003
2. Suster S, Moran CA. Histologic classification of thymoma: the World Health Organization and beyond. *Hematol Oncol Clin North Am* 2008; **22**: 381–92. doi: https://doi.org/10.1016/j.hoc.2008.03.001
3. Qu YJ, Liu GB, Shi HS, Liao MY, Yang GF, Tian ZX. Preoperative CT findings of thymoma are correlated with postoperative Masaoka clinical stage. *Acad Radiol* 2013; **20**: 66–72. doi: https://doi.org/10.1016/j.acra.2012.08.002
4. Abdel Razek AA, Khairy M, Nada N. Diffusion-weighted MR imaging in thymic epithelial tumors: correlation with World Health Organization classification and clinical staging. *Radiology* 2014; **273**: 268–75. doi: https://doi.org/10.1148/radiol.14131643
5. Razek AA, Elmorsy A, Elshafey M, Elhadedy T, Hamza O. Assessment of mediastinal tumors with diffusion-weighted single-shot echo-planar MRI. *J Magn Reson Imaging* 2009; **30**: 535–40. doi: https://doi.org/10.1002/jmri.21871
6. Li GF, Duan SJ, Yan LF, Wang W, Jing Y, Yan WQ, et al. Intravoxel incoherent motion diffusion-weighted MR imaging parameters predict pathological classification in thymic epithelial tumors. *Oncotarget* 2017; **8**: 44579–92. doi: https://doi.org/10.18632/oncotarget.17857
7. Yabuuchi H, Matsuo Y, Abe K, Baba S, Sunami S, Kamitani T, et al. Anterior mediastinal solid tumours in adults: characterisation using dynamic contrast-enhanced MRI, diffusion-weighted MRI, and FDG-PET/CT. *Clin Radiol* 2015; **70**: 1289–98. doi: https://doi.org/10.1016/j.crad.2015.07.004
8. Priola AM, Priola SM, Ciccone G, Evangelista A, Cataldi A, Gned D, et al. Differentiation of rebound and lymphoid thymic hyperplasia from anterior mediastinal tumors with dual-echo chemical-shift MR imaging in adulthood: reliability of the chemical-shift ratio and signal intensity index. *Radiology* 2015; **274**: 238–49. doi: https://doi.org/10.1148/radiol.14132665
9. Gümüştaş S, Inan N, Sarisoy HT, Anik Y, Arslan A, Ciftçi E, et al. Malignant versus benign mediastinal lesions: quantitative assessment with diffusion weighted MR imaging. *Eur Radiol* 2011; **21**: 2255–60. doi: https://doi.org/10.1007/s00330-011-2180-9
10. Abdel Razek AA, Soliman N, Elashery R. Apparent diffusion coefficient values of mediastinal masses in children. *Eur J Radiol* 2012; **81**: 1311–4. doi: https://doi.org/10.1016/j.ejrad.2011.03.008

11. Yabuuchi H, Matsuo Y, Abe K, Baba S, Sunami S, Kamitani T, et al. Anterior mediastinal solid tumours in adults: characterisation using dynamic contrast-enhanced MRI, diffusion-weighted MRI, and FDG-PET/CT. *Clin Radiol* 2015; **70**: 1289–98. doi: https://doi.org/10.1016/j.crad.2015.07.004
12. Just N. Improving tumour heterogeneity MRI assessment with histograms. *Br J Cancer* 2014; **111**: 2205–13. doi: https://doi.org/10.1038/bjc.2014.512
13. Xu XQ, Li Y, Hong XN, Wu FY, Shi HB. Radiological indeterminate vestibular schwannoma and meningioma in cerebellopontine angle area: differentiating using whole-tumor histogram analysis of apparent diffusion coefficient. *Int J Neurosci* 2017; **127**: 183–90. doi: https://doi.org/10.3109/00207454.2016.1164157
14. Rozenberg R, Thornhill RE, Flood TA, Hakim SW, Lim C, Schieda N. Whole-tumor quantitative apparent diffusion coefficient histogram and texture analysis to predict gleason score upgrading in intermediate-risk 3 + 4 = 7 prostate cancer. *AJR Am J Roentgenol* 2016; **206**: 775–82. doi: https://doi.org/10.2214/AJR.15.15462
15. Wu CJ, Wang Q, Li H, Wang XN, Liu XS, Shi HB, et al. DWI-associated entire-tumor histogram analysis for the differentiation of low-grade prostate cancer from intermediate-high-grade prostate cancer. *Abdom Imaging* 2015; **40**: 3214–21. doi: https://doi.org/10.1007/s00261-015-0499-4
16. Xu XQ, Hu H, Su GY, Zhang L, Liu H, Hong XN, et al. Orbital indeterminate lesions in adults: combined magnetic resonance morphometry and histogram analysis of apparent diffusion coefficient maps for predicting malignancy. *Acad Radiol* 2016; **23**: 200–8. doi: https://doi.org/10.1016/j.acra.2015.10.015
17. Xu XQ, Hu H, Su GY, Liu H, Hong XN, Shi HB, et al. Utility of histogram analysis of ADC maps for differentiating orbital tumors. *Diagn Interv Radiol* 2016; **22**: 161–7. doi: https://doi.org/10.5152/dir.2015.15202
18. Lu SS, Kim SJ, Kim N, Kim HS, Choi CG, Lim YM. Histogram analysis of apparent diffusion coefficient maps for differentiating primary CNS lymphomas from tumefactive demyelinating lesions. *AJR Am J Roentgenol* 2015; **204**: 827–34. doi: https://doi.org/10.2214/AJR.14.12677
19. DeLong ER, DeLong DM, Clarke-Pearson DL. Comparing the areas under two or more correlated receiver operating characteristic curves: a nonparametric approach. *Biometrics* 1988; **44**: 837–45. doi: https://doi.org/10.2307/2531595
20. Xu XQ, Ma G, Wang YJ, Hu H, Su GY, Shi HB, et al. Histogram analysis of diffusion kurtosis imaging of nasopharyngeal carcinoma: correlation between quantitative parameters and clinical stage. *Oncotarget* 2017; **8**: 47230–8. doi: https://doi.org/10.18632/oncotarget.17591
21. Kang Y, Choi SH, Kim YJ, Kim KG, Sohn CH, Kim JH, et al. Gliomas: histogram analysis of apparent diffusion coefficient maps with standard- or high-b-value diffusion-weighted MR imaging--correlation with tumor grade. *Radiology* 2011; **261**: 882–90. doi: https://doi.org/10.1148/radiol.11110686